DNA Binding to Mica Correlates with Cationic Radius: Assay by Atomic Force Microscopy

Helen G. Hansma and Daniel E. Laney
Department of Physics, University of California, Santa Barbara, California 93106

ABSTRACT In buffers containing selected transition metal salts, DNA binds to mica tightly enough to be directly imaged in the buffer in the atomic force microscope (AFM, also known as scanning force microscope). The binding of DNA to mica, as measured by AFM-imaging, is correlated with the radius of the transition metal cation. The transition metal cations that effectively bind DNA to mica are Ni(II), Co(II), and Zn(II), which have ionic radii from 0.69 to 0.74 Å. In Mn(II), ionic radius 0.82 Å, DNA binds weakly to mica. In Cd(II) and Hg(II), respective ionic radii of 0.97 and 1.1 Å, DNA does not bind to mica well enough to be imaged with the AFM. These results may to relate to how large a cation can fit into the cavities above the recessed hydroxyl groups in the mica lattice, although hypotheses based on hydrated ionic radii cannot be ruled out. The dependence of DNA binding on the concentrations of the cations Ni(II), Co(II), or Zn(II) shows maximal DNA binding at ~1-mM cation. Mg(II) does not bind DNA tightly enough to mica for AFM imaging. Mg(II) is a Group 2 cation with an ionic radius similar to that of Ni(II). Ni(II), Co(II), and Zn(II) have anomalously high enthalpies of hydration that may relate to their ability to bind DNA to mica. This AFM assay for DNA binding to mica has potential applications for assaying the binding of other polymers to mica and other flat surfaces.

INTRODUCTION

Atomic force microscopy (AFM) (Binnig et al., 1986; Rugar et al., 1990) is a useful new technique for imaging DNA and DNA-protein complexes in air and in aqueous solutions. The AFM images molecules on surfaces by raster-scanning a sharp tip back and forth across the surface. The tip is at the end of a cantilever that deflects as the tip encounters height changes on the sample surface. AFM images give topographic information about the sample surface, often at submolecular resolution.

AFM of DNA in air is a convenient alternative to electron microscopy for determining bend angles and other conformations of DNA and DNA-protein complexes (Rees et al., 1993; Erie et al., 1994; Hansma et al., 1994; Wyman et al., 1995). In aqueous solutions, DNA can be imaged at submolecular resolution in a physiological environment (Hansma et al., 1993; Lyubchenko et al., 1993b; Bezanilla et al., 1994a; Lyubchenko et al., 1993a). Even moving DNA molecules as short as 300 base pairs (bp) can sometimes be imaged by AFM in aqueous buffers (Bezanilla et al., 1994b; Hansma et al., 1995). Mica is common surface for AFM-imaging of DNA (Vesenka et al., 1992; Hansma et al., 1992; Bustamante et al., 1992; Schaper et al., 1993), although silylated mica and other surfaces have also been used (Lyubchenko et al., 1992; Hegner et al., 1993).

There are two ways of preparing DNA samples for AFM-imaging on mica: 1) by first drying the DNA onto mica, and 2) by imaging DNA solutions on mica. In the first way, a drop of DNA-containing solution is deposited onto freshly split mica, rinsed with water, and dried thoroughly. The DNA dried onto mica can then be imaged either in air or in fluid. In the second way, DNA in aqueous solutions can be imaged on mica in the AFM even without drying, if the solution contains Ni(II).

When DNA is dried onto mica, the amount of DNA bound to the mica is significantly greater when the DNA solution contains salts of a divalent or other multivalent inorganic cation, as compared with DNA in water. The inorganic cations that enhance DNA binding to mica include Mg(II), Ca(II), Ba(II), Co(II), Ni(II), Zn(II), Cr(II), La(III), and Zr(IV) (Vesenka et al., 1992; Thundat et al., 1992; Hansma et al., 1993). Basically, all of the multivalent inorganic cations that have been tested will increase the binding of DNA to mica. In contrast, monovalent cations such as K(I) decrease the binding of DNA to mica (Bezanilla et al., 1995).

The Group 2 cations Mg(II) and Ca(II) do not bind DNA in solution tightly enough to mica for AFM imaging without drying. Ni(II) is the only cation previously known to bind DNA to mica tightly enough for AFM imaging without drying (Bezanilla et al., 1994b).

This paper presents results from AFM-imaging of DNA in buffers containing other divalent inorganic cations and models that might explain these results. AFM-imaging of DNA solutions is a rapid, visual, semiquantitative method for assaying DNA binding to mica that may have applications to the binding of other polymers to mica and other smooth surfaces.

Received for publication 31 August 1995 and in final form 19 January 1996.

Address reprint requests to Dr. Helen G. Hansma, Department of Physics, University of California, Santa Barbara, CA 93106. Tel.:805-893-3881; Fax: 805-893-8315; E-mail: hhansma@physics.ucsb.edu.

0006-3495/96/04/1933/07 $2.00

MATERIALS AND METHODS

DNA solutions

For stable imaging, Figs. 1 and 2: The DNA, ϕX-174 RF DNA-*Hinc* II Digest (Pharmacia, Piscataway, NJ), contains DNA molecules of 10 different lengths ranging in size from 79 to 1057 bp, corresponding to lengths from ~25 to 350 nm. The DNA was diluted to 0.5 ng/μL in buffers

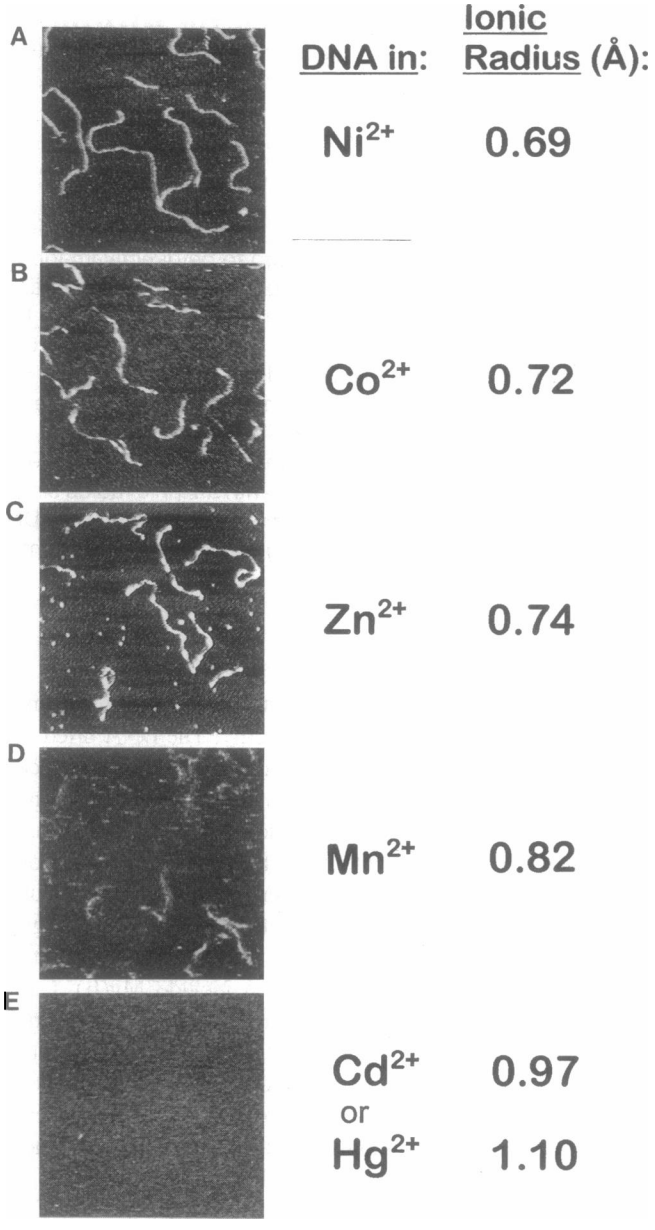

FIGURE 1 AFM images of DNA on mica in aqueous buffers containing 1 mM MCl_2, where M is *A*) Ni(II), *B*) Co(II), *C*) Zn(II), *D*) Mn(II), *E*) Cd(II) or Hg(II). Clear images of DNA on mica are seen in MCl_2 solutions where the ionic radius of M is 0.69 to 0.74 Å (Ni^{2+}, Co^{2+}, and Zn^{2+}). In Mn^{2+} (0.82-Å radius), DNA molecules bind weakly to mica and move during AFM imaging, whereas in Cd^{2+} or Hg^{2+}, DNA does not bind to mica well enough for AFM imaging. Images are 500 nm × 500 nm. The DNA is ϕX-174 *Hinc* II digest, containing DNA molecules 25 nm to 350 nm long. *C*) Dots in the image of DNA in Zn^{2+} are debris; this image was taken after the image in *B*, using the same cantilever, after rinsing with water. When imaging in fluid, debris is often seen, which can be minimized by thoroughly washing the fluid cell and using a new cantilever for each sample. *E*) Images of DNA in Mg(II) or Ca(II) also showed no DNA. Ionic radii are from (Pauling, 1960) and (Israelachvili, 1985).

containing 10 mM HEPES, pH 7, and 1 mM concentrations of one of the following salts: $MgCl_2$, $CaCl_2$, $MnCl_2$, $CoCl_2$, $NiCl_2$, $ZnCl_2$, $CdCl_2$, $HgCl_2$, or $CuCl_2$,. HEPES (N-[2-Hydroxyethyl]piperazine-N′-[2-ethanesulfonic acid]) was obtained from Sigma (St. Louis, MO).

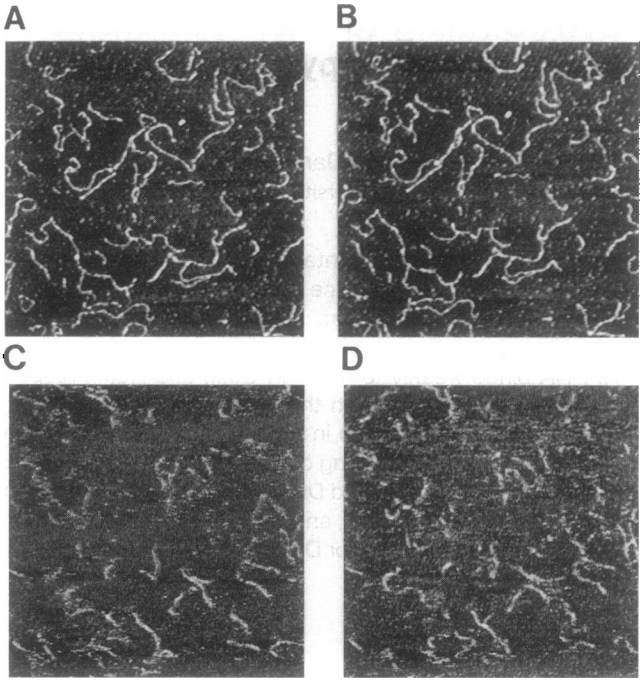

FIGURE 2 *A*, *B*) Reproducible images of DNA on mica in aqueous buffer containing $ZnCl_2$. These successive images were captured 1 min apart and ~10–15 min after pipetting the DNA solution onto the mica. *C*, *D*) In $MnCl_2$ solution, even the best DNA images are not reproducible. These successive images were captured 1 min apart and ~20–25 min after pipetting the DNA solution onto the mica. The DNA is ϕX-174 *Hinc* II digest, containing DNA molecules 25 to 350 nm long. Images are 1 μm × 1 μm.

For concentration dependence, Fig. 3: DNA of 324 bp prepared by polymerase chain reaction was diluted to 2 ng/μL or 3.3 ng/μL in buffer containing 5 mM HEPES, pH 7, and 0.1 to 20 mM $NiCl_2$, $CoCl_2$, or $ZnCl_2$.

For DNA movies, Fig. 4: DNA of 500 bp prepared by polymerase chain reaction from lambda DNA was diluted to 0.5 ng/μL in a buffer containing 5 mM HEPES, 5 mM KCl, 2 mM $MgCl_2$, pH 7.

Sample preparation

For stable imaging: The fluid cell with cantilever was inserted into the AFM over a mica surface, the cantilever was lowered to ~0.03 mm above the mica surface, and the head was leveled with a feeler gauge (see below). The fluid cell was then removed, and the mica was freshly cleaved with Scotch tape. The inlet and outlet ports of the fluid cell were plugged, and a 25-μL DNA-containing solution, as described above, was pipetted onto the cantilever in the fluid cell. The fluid cell with the DNA solution on it was inverted over the freshly cleaved mica surface for DNA imaging.

For DNA movies: Freshly cleaved mica was treated with 1 mM $CoCl_2$ and rinsed with water as described previously for $NiCl_2$ (Hansma et al., 1995). DNA solution was applied to the mica as described above for stable DNA imaging.

AFM-imaging

Tapping AFM in the DNA solution was done with a Nanoscope III with MultiMode AFM (Digital Instruments, Santa Barbara, CA). The cantilever was silicon nitride, 100-μ long, with narrow arms and an oriented twin tip designed to minimize double images of molecules < ~100 nm high (Digital Instruments, Santa Barbara, CA).

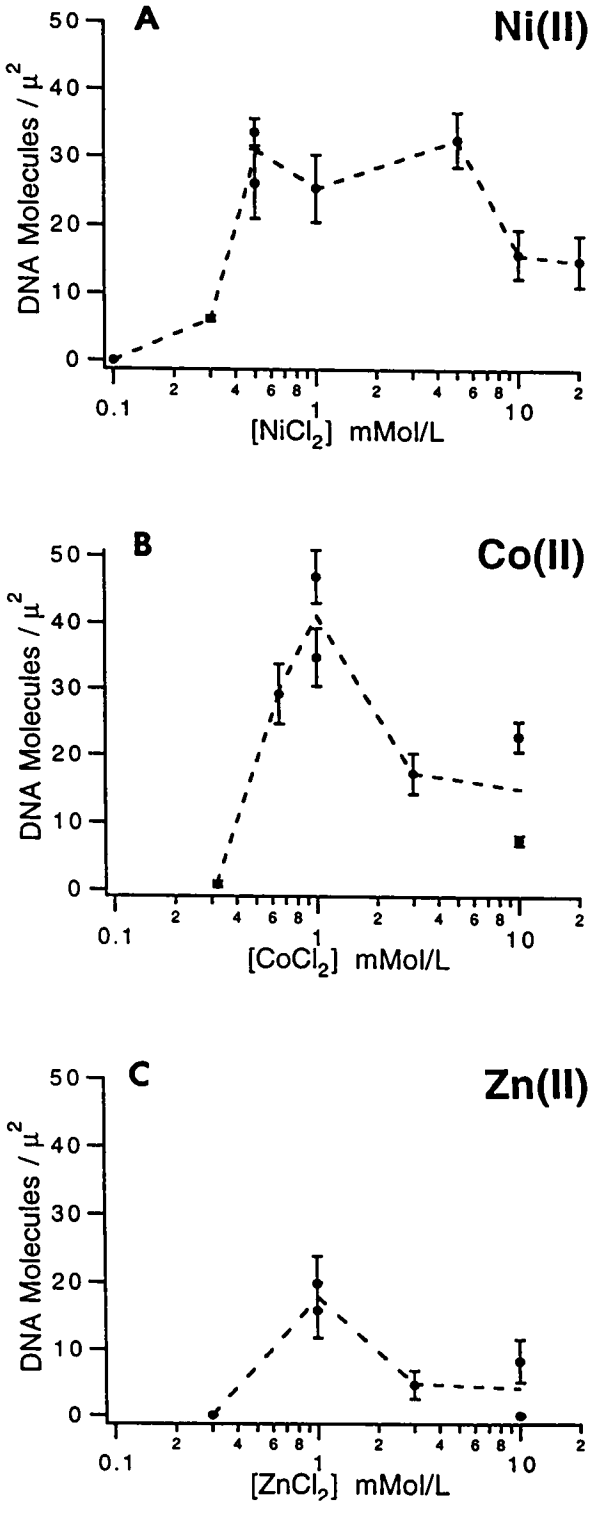

FIGURE 3 DNA binding to mica vs. concentration of the following divalent cations: *A*) Ni(II), *B*) Co(II), or *C*) Zn(II). Data points are means ± standard deviations for the number of 324-bp DNA molecules in three to seven different 1 μm × 1 μm scans in a single sample. The DNA density at a given concentration of divalent cation varies from sample to sample, as can be seen from concentrations with two data points, e.g., 0.5 mM Ni(II) (*A*) and 1 mM Co(II) (*B*). Data are for DNA concentrations of 2 ng/μL. In *B*, the actual DNA concentration was 3.3 ng/μL; data points in *B* are adjusted 2 ng/μL, assuming a linear relationship between DNA concentration and DNA binding to mica over this concentration range.

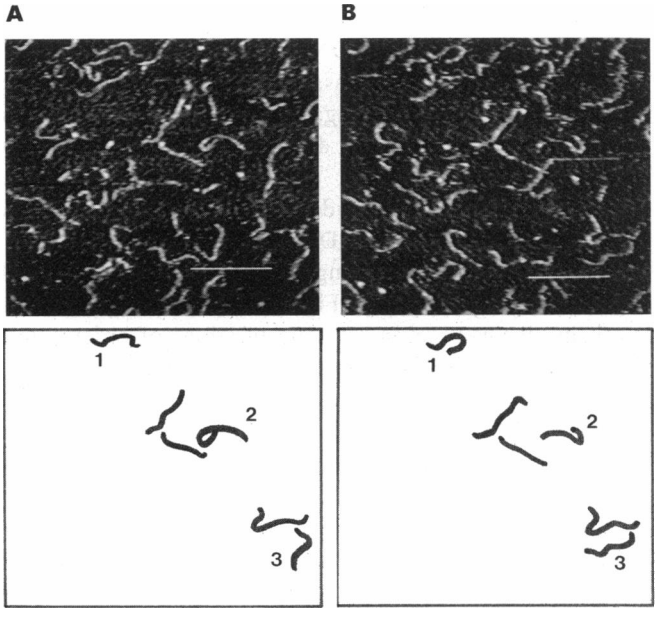

FIGURE 4 DNA molecules, 500 bp, in motion on Co(II)-treated mica in a buffer containing no Co(II). Scan rate, 7.3 Hz; 256 samples. *A*, *B*) Images were captured 3 min apart. Drawings show positions of selected molecules in the two images. Numbered molecules show significant movement between images. Scale bars are 200 nm.

Leveling the AFM head is important so that only the tip is in contact with the sample surface. The AFM head can be leveled by adjusting it so that the gap between the AFM head and the AFM base is the same by each of the three set screws. The heights of these gaps can be measured with a 16-piece feeler gauge assortment of flat metal strips (McMaster-Carr, Los Angeles, CA), and the sizes of the gaps can be adjusted with the set screws until they are all equal.

RESULTS

DNA in solution adsorbs rapidly to mica and tightly enough to be imaged by AFM if the solution contains Ni(II), Co(II), or Zn(II) (Fig. 1, *A-C*).

In solutions containing Mn(II), a few DNA molecules sometimes temporarily bind tightly enough to the mica to be imaged (Fig. 1 *D*). Unlike DNA in Ni(II), Co(II) or Zn(II), which can be imaged repeatedly without moving (Fig. 2, *A* and *B*) (Bezanilla et al., 1994b), DNA in Mn(II) usually shows significant movement from image to image (Fig. 2, *C* and *D*). Often after a few minutes of imaging, no DNA can be seen on the mica surface in Mn(II).

In solutions containing Cd(II), Hg(II) (Fig. 1 *E*), Mg(II), or Ca(II), DNA does not bind to mica tightly enough for AFM-imaging in solution. With DNA solutions containing Cu(II), AFM images showed lumps instead of DNA strands.

There is no significant difference in the amount of DNA bound to mica in 1 mM Ni(II), Co(II), and Zn(II) in repeated experiments of the type shown in Fig. 1. There is considerable variability in the amount of DNA bound to mica in different experiments with the same cation. This variability between experiments in the amount of DNA bound is

greater than the variability among cations in the amount of DNA bound. Because the DNA ϕX-174 *Hinc* II digest has molecules of many lengths, it is not easy to precisely quantitate the DNA binding, but a qualitative ranking of DNA binding supports the above observations, as can be seen also from Fig. 1, *A-C*.

The cation concentration dependence of DNA binding to mica was investigated for DNA in M(II), where M(II) is Ni(II), Co(II), or Zn(II), using DNA of constant length (324 bp) for easier quantitation (Fig. 3). DNA binding showed a peak in all three cations at concentrations of order 1 mM M(II). No DNA binding was observed at 0.1 mM M(II), and DNA binding was in all cases lower at 10 mM M(II) than at 1 mM M(II). The cation concentration range for maximum DNA binding appears to be broader for Ni(II) than for Co(II) or Zn(II) (Fig. 3).

Data are means $\pm$ standard deviations for scans of different areas of the same sample. The variability between samples, as mentioned in the preceding paragraph, can be seen quantitatively in Fig. 3 for M(II) concentrations with two data points, such as 5 mM Ni(II) (Fig. 3 *A*) or 1 mM Co(II) (Fig. 3 *B*).

The amount of DNA bound is also dependent on the DNA concentration. A high concentration of DNA in 1 mM Co(II) gave very dense fields of DNA on mica. With a low concentration of DNA, few molecules were seen; but there were only 60% as many DNA molecules in 10 mM Co(II) as in 1 mM Co(II), which is similar to Fig. 3 *B*.

Rates of DNA binding to mica cannot be measured, because DNA binding is complete within 5 to 10 min, which is usually as soon as images can be taken. The earliest images do not tend to show less DNA bound, but rather weaker DNA binding; i.e., images in the first 5 to 10 min sometimes show less stable DNA imaging.

When DNA in a buffer without transition metal cation was pipetted onto mica rinsed with $CoCl_2$, the DNA molecules could be imaged fairly well even when they were moving on the mica surface (Fig. 4). The molecules numbered 1, 2, and 3 showed clear movement between the two images. These results are similar to the results reported previously for DNA on Ni(II)-mica (Bezanilla et al., 1994b; Hansma et al., 1995).

DISCUSSION

Correlation between DNA binding to mica and cationic radius

DNA binding to mica correlates well with the ionic radius of the transition metal cation present in the buffer. When the ionic radius is 0.74 Å or less, DNA binds tightly to mica, such that DNA in solution can be imaged directly in the AFM.

Mica is a layered mineral with a negative surface charge, and DNA is a negatively charged polymer. Thus, divalent cations probably bind DNA to mica by bridging the negative charges on the DNA and the mica.

The correlation of DNA binding with cationic radius could be due to the steric requirements of either the DNA or the mica. Research on mica suggests that the mica structure, not the DNA structure, induces the results observed here for transition metal cations.

The mica surface has silicon, oxygen, and aluminum atoms surrounding hydroxyl groups that are recessed slightly below the surface. These recessed hydroxyl groups have a hexagonal arrangement and a spacing of 0.5 nm. There is evidence that H_3O^+ (Claesson et al., 1986) and other small cations (Nishimura et al., 1995) can adsorb into the mica surface at the sites of these recessed hydroxyl groups ("cavities").

Transition metal cations on mica have not been investigated previously, but among the Group 2 cations that have been investigated, only Mg(II) has a radius small enough to enter the mica cavities (Nishimura et al., 1995). Mg(II) has an ionic radius of 0.65 Å, similar to that of Ni(II), Co(II), and Zn(II). Thus it is possible that these transition metal cations can bind DNA to mica because they are small enough to fit into the mica cavities.

Ca(II), which is too large to fit easily into the mica cavities (Nishimura et al., 1995), has an ionic radius of 0.99 Å. Cd(II) and Hg(II), with ionic radii similar to Ca(II), cannot bind DNA in solution to mica well enough for AFM imaging; whereas Mn(II), with an intermediate ionic radius (0.82 Å) is intermediate in its ability to bind DNA to mica in the AFM (Fig. 1).

From the above discussion, one would expect Mg(II) to bind DNA to mica well enough for AFM-imaging in solution because its ionic radius is similar to those of Ni(II), Co(II), and Zn(II), but it does not. There are several possible explanations for the inability of Mg(II) to bind DNA in solution to mica.

Hydrated Mg(II) has a slow turnover of water molecules, 10^5/s, as compared with other ions such as Ca(II), K(I), and Na(I), whose water substitution rates are 10^8 to 10^9 water molecules/s (Hille, 1992). But Ni(II) has an even slower water substitution rate, 10^4/s. And the water substitution rate for Zn(II), which can bind DNA well to mica, is intermediate between those of Mn(II),$\sim 5 \times 10^6$/s, and Cd(II),$\sim 5 \times 10^8$/s, both of which do not bind DNA well to mica. Thus, the water substitution rates of cations do not correlate with the cations' effects on the binding of DNA to mica.

Two characteristics do distinguish Mg(II) from Ni(II), Co(II), and Zn(II). One is the position of the cations in the periodic table. Mg(II) is a Group 2 metal with p electrons in its outer orbital, whereas Ni(II), Co(II), and Zn(II) are transition metals with d electrons in their outer orbitals. Mg(II) can form very few complexes in aqueous solution except for complexes with polyphosphate anions and chelating ligands such as EDTA. Divalent transition metal cations can form a wider range of complexes in aqueous solutions (Sharpe, 1986).

The second difference between Mg(II) and the transition metal cations Ni(II), Co(II), and Zn(II) is that the transition

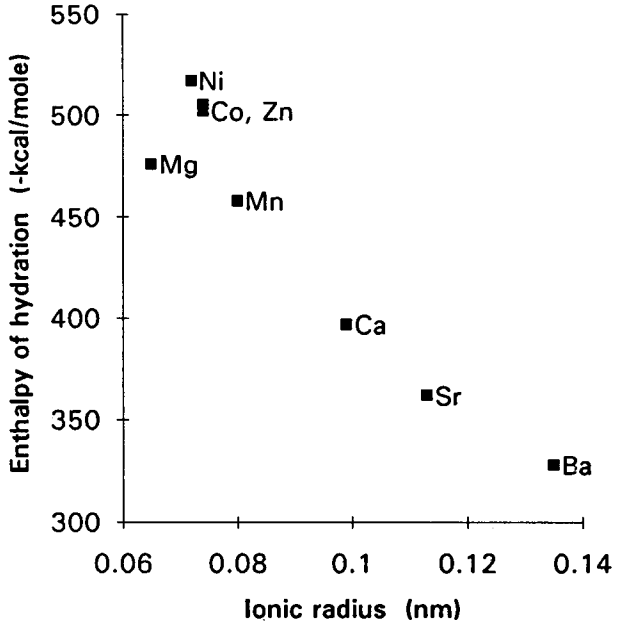

FIGURE 5 Enthalpies of hydration vs. cationic radii for the divalent cations shown above. Enthalpies of hydration (Hille, 1992) correlate well with cationic radii for Group 2 cations and Mn(II). The anomalously high enthalpies of hydration for Ni(II), Co(II), and Zn(II) may relate to their ability to bind DNA tightly to mica.

metal cations have higher enthalpies of hydration (Hille, 1992). There is a good linear relationship between the enthalpy of hydration and the ionic radius for Mn(II) and the group 2 cations, whereas Ni(II), Co(II), and Zn(II) have anomalously high enthalpies of hydration (Fig. 5). One might expect a high enthalpy of hydration to decrease the cation's ability to complex with DNA and mica because of the stability of the hydrated ion. In view of the AFM data, however, it appears that the high enthalpies of hydration may reflect the ability of Ni(II), Co(II), and Zn(II) to form strong complexes with ligands other than water as well.

The observed differences between Mg(II) and Ni(II), Co(II), or Zn(II) do not seem to come from differences in their binding to DNA. Cations can bind to either the phosphate backbone or the bases of DNA. Cations that stabilize the DNA double helix by bridging phosphate groups raise the DNA's melting temperature. Cations that destabilize the double helix by binding to DNA bases lower the melting temperature (Barton et al., 1980; Saenger, 1984). According to this melting-temperature assay, Mg(II) binds to DNA phosphate groups, and the affinity of divalent cations for DNA bases increases along this series: Mg(II), Co(II), Ni(II), Mn(II), Zn(II), Cd(II), and Cu(II) (whose radius is 0.73 Å) (Barton et al., 1980; Saenger, 1984). This series shows no correlation with ionic radius or with ability to bind DNA to mica.

Although DNA in Mg(II) solutions does not bind to mica strongly enough for AFM imaging in solution, there is evidence that DNA in Mg(II) solutions binds weakly to mica. This evidence comes from AFM images of DNA dried onto mica. DNA in Mg(II) solutions can be pipetted onto mica, rinsed with water, dried, and seen in the AFM. As described in the Introduction, all the divalent inorganic cations that have been tested can increase the amount of DNA bound to mica, as assayed by AFM of DNA dried onto mica. Perhaps Mg(II) can bind DNA to mica electrostatically by cross-bridging the negatively charged DNA and mica. Mg(II) and other divalent and even monovalent cations are known to be able to neutralize the mica surface (Pashley et al., 1984; G. L. Gaines, 1957). In addition, Ni(II), Co(II), and Zn(II) can perhaps bind DNA more tightly to mica by some more specific interaction, such as insertion into the mica cavities.

Alternatively, the DNA-binding properties of these cations may be related to some other property, such as their hydrated radii. The hydrated radii for divalent cations are inversely proportional to their crystal radii (Israelachvili, 1985). Interaction forces between mica sheets in ionic solutions are consistent with the presence of hydrated cations, but only Group 1 and Group 2 cations have thus far been studied (Pashley et al., 1984; Pashley, 1981).

Dependence of DNA binding to mica on cationic concentrations

The cations Ni(II), Co(II), and Zn(II), hereafter called M(II), have another interesting effect on DNA binding to mica. DNA binding as a function of M(II) concentration shows a peak at ~1 mM M(II) for all three M(II), falling off to zero DNA bound at 0.1 mM M(II) and to ~50% of the maximal DNA binding at 10 mM M(II) (Fig. 3). At higher concentrations of DNA, the mica surface can become covered with DNA (data not shown).

At 0.1 mM M(II), there may be too small a density of M(II) on the mica surface for DNA binding. It is less clear why DNA binding to mica decreases in 10 mM M(II). A mass action view of the sample in 10 mM M(II) suggests that as the concentration of M(II) increases, both DNA and mica will become saturated with M(II), and the probability will decrease that single M(II) ions will bridge both the DNA and the mica. A steric view of the sample suggests that the spacing of charges on DNA and mica may affect binding. Phosphate groups on DNA have a spacing of 0.3 nm, whereas the mica lattice spacing is 0.5 nm. Thus the optimal binding of DNA to mica might occur with 1 M(II) ion/nm DNA, where every third DNA base could bind to every second mica site. With more than 1 M(II) ion/nm, DNA binding to mica might decrease. Thus, both steric effects and mass action effects can explain the decreased DNA binding seen in 10 mM N(II).

The surface charge on mica, in the absence of counterions, is two negative charges per nm^2 (Pashley et al., 1984). Under the experimental conditions used in Fig. 3, there are 10^{14} negative charges on mica covered by a solution layer 0.6 mm thick containing 10^{14} nucleotides of DNA and, at 1

mM M(II), 10^{16} M(II). DNA binding at a level of 30 molecules/μm^2 corresponds to 10^{12} nucleotides of DNA bound to the surface area of the mica under the solution.

Changes in the surface potential on mica should affect DNA binding to mica. In low concentrations of Na^+, the surface potential of mica unexpectedly becomes more negative (Pashley, 1981). This has been explained with a mass action model of competition between hydrated Na^+ and H_3O^+, with H_3O^+ having a higher affinity for mica and hydrated Na^+ being so large that it overlaps sites on mica adjacent to the one at which it is binding.

Mica's surface potentials have not yet been measured in Ni(II), Co(II), or Zn(II), and our hypothesis predicts that these cations can dehydrate when binding to mica. But mica's high affinity for H^+ could explain the large decrease in DNA binding to mica concentrations of less than 1 mM Ni(II), Co(II), or Zn(II). A pH dependence of DNA binding to mica has been seen under the conditions used for making DNA movies, where there is ~25% less DNA on the mica at pH 7 than at pH 8 (D. E. Laney, unpublished results).

Mobile DNA molecules

When the DNA solution does not contain Ni(II) but the mica has been rinsed with Ni(II), some of the DNA molecules move on the mica surface in such a way that they can be imaged in changing positions in the AFM, giving time-lapse DNA movies (Bezanilla et al., 1994b; Hansma et al., 1995; Hansma et al., 1996). DNA on Co(II)-mica can also be imaged in motion, as shown in Fig. 3. Thus Co(II) resembles Ni(II) both in its ability to bind DNA tightly to mica and in its ability to bind DNA loosely to mica. We do not yet know whether DNA in motion can be imaged on Zn(II)-rinsed mica.

It is difficult to quantitate DNA in motion. Most clear images of moving molecules are for movement in the fast scan direction (horizontal movement) or for tethered molecules, where movement is restricted. The moving molecules highlighted in Fig. 4 are all tethered (molecules 1, 2, and 3). Molecules moving in the slow scan direction (vertical movement) are less likely to give clear images of intact full length molecules, because successive points on a vertical line are imaged at relatively long intervals,~0.1 s, under typical imaging conditions. In contrast, successive points on a horizontal line are imaged at intervals < 1 ms. Some of the broken or short molecules in Fig. 3 may be molecules moving in the slow scan direction; others may be molecules bound too weakly to the mica surface for good imaging.

AFM images of mobile DNA molecules are being used to measure the persistence lengths, or stiffness, of individual small DNA molecules in solution at room temperature (Hansma et al., 1996); this has not previously been possible.

CONCLUSION

DNA in solutions containing divalent transition metal cations binds to mica tightly enough for AFM imaging if the ionic radius of the transition metal cation is 0.69 to 0.74 Å. One possible explanation for these results is that small transition metal cations can fit into the cavities above the recessed hydroxyl groups on the mica surface, although other explanations involving hydrated cations cannot be excluded.

The Group 1 cation Mg(II) does not bind DNA tightly to mica even though its ionic radius is also small, 0.65 Å. The cations that bind DNA well to mica, Ni(II), Co(II), and Zn(II) have anomalously high enthalpies of hydration in relation to their ionic radii. These high enthalpies of hydration may reflect the ability of Ni(II), Co(II), and Zn(II) to form unusually strong complexes with other ligands such as DNA and mica as well.

Maximum DNA binding to mica is observed in ~1 mM Ni(II), Co(II), or Zn(II). This AFM assay for DNA binding may also be a good way for assaying the binding of other polymers to mica under different conditions.

We thank Andrew Gewirth, Carol Vandenberg, Jacob Israelachvili, Bettye Smith, Allison Butler, Robert Sinsheimer, and Paul Hansma for helpful discussions; Mikhail Kashlev and Evgeny Nudler for providing the 324-bp DNA; Kerry Kim for preparing the 500 bp DNA; David Vie and Nazanin Firouz for expert technical assistance; Rudi Stuber for suggesting the use of a feeler gauge for leveling the AFM; and Virgil Elings and Mark Wendman of Digital Instruments for designing the oriented twin tips. This work was supported by NSF MCB 9317466 and Digital Instruments.

REFERENCES

Barton, J. K., and S. J. Lippard. 1980. Heavy metal interactions with nucleic acids. *In* Nucleic Acid-Metal Ion Interactions. John Wiley and Sons, New York. 31–113.

Bezanilla, M., C. Bustamante, and H. G. Hansma. 1994a. Improved visualization of DNA in aqueous buffer with the atomic force microscope. *Scanning Microsc.* 7:1145–1148.

Bezanilla, M., B. Drake, E. Nudler, M. Kashlev, P. K. Hansma, and H. G. Hansma. 1994b. Motion and enzymatic degradation of DNA in the atomic force microscope. *Biophys. J.* 67:2454–2459.

Bezanilla, M., S. Manne, D. E. Laney, Y. L. Lyubchenko, and H. G. Hansma. 1995. Adsorption of DNA to mica, silylated mica and minerals: characterization by atomic force microscopy. *Langmuir.* 11:655–659.

Binnig, G., C. F. Quate, and C. Gerber. 1986. Atomic force microscope. *Phys. Rev. Lett.* 56:930–933.

Bustamante, C., J. Vesenka, C. L. Tang, W. Rees, M. Guthold, and R. Keller. 1992. Circular DNA molecules imaged in air by scanning force microscopy. *Biochemistry.* 31:22–6.

Claesson, P. M., P. Herder, P. Stenius, J. C. Eriksson, and R. M. Pashley. 1986. An ESCA and AES study of ion-exchange on the basal plane of mica. *J. Colloid Interface Sci.* 109:31–39.

Erie, D. A., G. Yang, H. C. Schultz, and C. Bustamante. 1994. DNA bending by Cro protein in specific and nonspecific complexes: implications for protein site recognition and specificity. *Science.* 266: 1562–1566.

G. L. Gaines, Jr. 1957. The ion-exchange properties of muscovite mica. *J. Phys. Chem.* 61:1408–1413.

Hansma, H. G., M. Bezanilla, D. L. Laney, R. L. Sinsheimer, and P. K. Hansma. 1995. Applications for atomic force microscopy of DNA. *Biophys. J.* 68:1672–1677.

Hansma, H. G., M. Bezanilla, F. Zenhausern, M. Adrian, and R. L. Sinsheimer. 1993. Atomic force microscopy of DNA in aqueous solutions. *Nucleic Acids Res.* 21:505–512.

Hansma, H. G., K. A. Browne, M. Bezanilla, and T. C. Bruice. 1994. Bending and straightening of DNA induced by the same ligand: characterization with the atomic force microscope. *Biochemistry.* 33: 8436–8441.

Hansma, H. G., D. E. Laney, I. Revenko, K. Kim, and J. P. Cleveland. 1996. Bending and motion of DNA in the atomic force microscope. *In* Ninth Conversation in Biomolecular Stereodynamics. Adenine Press, Albany, NY. In press.

Hansma, H. G., J. Vesenka, C. Siegerist, G. Kelderman, H. Morrett, R. L. Sinsheimer, C. Bustamante, V. Elings, and P. K. Hansma. 1992. Reproducible imaging and dissection of plasmid DNA under liquid with the atomic force microscope. *Science.* 256:1180–1184.

Hegner, M., P. Wagner, and G. Semenza. 1993. Immobilizing DNA on gold via thiol modification for atomic force microscopy imaging in buffer solutions. *FEBS Letters.* 336:452–456.

Hille, B. 1992. Ionic Channels of Excitable Membranes. Sinauer Associates Inc., Sunderland, Massachusetts.

Israelachvili, J. N. 1985. Intermolecular and Surface Forces with Applications to Colloidal and Biological Systems. Academic Press, New York.

Lyubchenko, Y. L., A. A. Gall, L. S. Shlyakhtenko, R. E. Harrington, B. L. Jacobs, P. I. Oden, and S. M. Lindsay. 1992. Atomic force microscopy imaging of double stranded DNA and RNA. *J. Biomol. Struct. Dyn.* 10:589–606.

Lyubchenko, Y. L., P. I. Oden, D. Lampner, S. M. Lindsay, and K. A. Dunker. 1993a. Atomic force microscopy of DNA and bacteriophage in air, water and propanol: the role of adhesion forces. *Nucleic Acids Res.* 21:1117–23.

Lyubchenko, Y. L., L. S. Shlyakhtenko, R. E. Harrington, P. I. Oden, and S. M. Lindsay. 1993b. Atomic force microscopy of long DNA: imaging in air and under water. *Proc. Natl. Acad. Sci.* 90:2137–2140.

Nishimura, S., P. J. Scales, H. Tateyama, K. Tsunematsu, and T. W. Healy. 1995. Cationic modification of muscovite mica: an electrokinetic study. *Langmuir.* 11:291–295.

Pashley, R. M. 1981. DLVO and hydration forces between mica surfaces in Li^+, Na^+, K^+, and Cs^+ electrolyte solutions: a correlation of double-layer and hydration forces with durface cation exchange properties. *J. Colloid Interface Sci.* 83:531–546.

Pashley, R. M., and J. N. Israelachvili. 1984. DLVO and hydration forces between mica surfaces in Mg^{2+}, Ca^{2+}, Sr^{2+}, and Ba^{2+} chloride solutions. *J. Colloid Interface Sci.* 97:446–455.

Pauling, L. 1960. The Nature of the Chemical Bond. Cornell University Press, Ithaca, New York.

Rees, W. A., R. W. Keller, J. P. Vesenka, C. Yang, and C. Bustamante. 1993. Evidence of DNA bending in transcription complexes imaged by scanning force microscopy. *Science.* 260:1646–1649.

Rugar, D., and P. K. Hansma. 1990. Atomic force microscopy. *Phys. Today.* 43:23–30.

Saenger, W. 1984. Principles of Nucleic Acid Structure. Springer-Verlag, New York.

Schaper, A., L. I. Pietrasanta, and T. M. Jovin. 1993. Scanning force microscopy of circular and linear DNA spread on mica with a quaternary ammonium salt. *Nucleic Acids Research.* 21:6004–6009.

Sharpe, A. G. 1986. Inorganic Chemistry. Longman, New York.

Thundat, T., D. P. Allison, R. J. Warmack, G. M. Brown, K. B. Jacobson, J. J. Schrick, and T. L. Ferrell. 1992. Atomic force microscopy of DNA on mica and chemically modified mica. *Scanning Microsc.* 6:911–918.

Vesenka, J., M. Guthold, C. L. Tang, D. Keller, E. Delaine, and C. Bustamante. 1992. A substrate preparation for reliable imaging of DNA molecules with the scanning force microscope. *Ultramicroscopy.* 42–44: 1243–1249.

Wyman, C., E. Grotkopp, C. Bustamante, and H. C. M. Nelson. 1995. Determination of heat-shock transcription factor 2 stoichiometry at looped DNA complexes using scanning force microscopy. *EMBO Journal.* 14:117–123.